Polymeric Particles with Structural Complexity from Stable Immobilized Emulsions

ARTICLE *in* CHEMISTRY OF MATERIALS · SEPTEMBER 2007

Impact Factor: 8.35 · DOI: 10.1021/cm0708362

Polymeric Particles with Structural Complexity from Stable Immobilized Emulsions

Shin-Hyun Kim,[†] Chul-Joon Heo,[†] Su Yeon Lee,[†] Gi-Ra Yi,*[,‡] and Seung-Man Yang*[,†]

National Creative Research Initiative Center for Integrated Optofluidic Systems and Department of Chemical and Biomolecular Engineering, Korea Advanced Institute of Science and Technology, Daejeon, 305-701 Korea, and Nano-Bio System Research Team, Seoul Center, Korea Basic Science Institute, Seoul 136-713 Korea

Received March 27, 2007. Revised Manuscript Received July 1, 2007

We prepared polymeric structures with unusual complexity in surface morphology derived from photocurable emulsion droplets dispersed in an aqueous medium. The emulsion droplets a few tens of micrometers in size were stabilized with relatively small hydrophobic particles that were bound to the emulsion interfaces. The particle binding tended to immobilize the oil-in-water emulsion interface and dramatically increased the structural relaxation time of the interface deformation over a few days relative to a few milliseconds for an otherwise clean interface. In particular, perfectly immobilized emulsion drops maintained nonspherical elongated structures that were formed by shear-induced emulsification and could not be relaxed to a spherical shape. This property is useful for broad research areas ranging from crystallography and buckling phenomena to materials fabrication. The configuration of small particles on the interface and the "raspberry" shape of particle-stabilized emulsions were captured successfully by photocuring the emulsion droplets because the small bound particles immobilized the emulsion droplets. By selectively removing the small particles from the particle-covered polymeric structures, we prepared dimpled microparticles with various shapes. The dimple geometry depended on the interfacial properties or phase affinity of the small particles. The contact angle and binding energy of the particles were calculated on the basis of the dimple geometry. In addition, buckling phenomena of the particle-stabilized emulsions were observed when volatile oil was added to the photocurable resin.

Introduction

Colloidal spheres absorbed at liquid−liquid interface can form two-dimensional (2D) ordered structures by self-organization as they form 3D colloidal crystals in the bulk phase. Recent interest in 2D sphere packing at a spherical interface stems from its relevance to drug delivery, spherical crystallography, and materials science.[1−3] However, sphere packings in 2D arrangement at a liquid−liquid interface have not been fully understood relative to 3D sphere packings. In particular, 2D arrangement of spheres at the spherical interface of droplets has been known as Thompson's problem for a century and was analyzed by the classical Euler theorem.[4−6] Experimentally, Bausch et al. explored this packing problem using particle-stabilized emulsions or Pickering emulsions as a model system for spherical crystallography,[2,7] which have unique properties unlike those of surfactant stabilized emulsions as reported by Binks et al.[3,8−11] By evaporating the emulsion drop phase, the particle-stabilized emulsions were used to produce so-called "colloidosomes," which are selectively permeable capsules of rigid colloidal shells. Liposomelike colloidosomes can serve as drug carriers because of the structural advantages of a shell composed of particles.[1,12−15] Usually, the colloidal shells are unstable against disassembly during evaporation of the liquid inside emulsion drops, and a protein adhesion, annealing, gelation, or polymerization should be performed in order to attain enhanced mechanical strength.[1,12−18] Recently, spherical or rodlike colloids have been used for super-stabilization of foams[19−21] and photo-cross-linkable,

* Corresponding author. E-mail: smyang@kaist.ac.kr (S.-M.Y.); yigira@kbsi.re.kr (G.-R.Y.).
[†] Korea Advanced Institute of Science and Technology.
[‡] Korea Basic Science Institute.

(1) Dinsmore, A. D.; Hsu, M. F.; Nikolaides, M. G.; Marques, M.; Bausch, A. R.; Weitz, D. A. *Science* **2002**, *298*, 1006−1009.
(2) Bausch, A. R.; Bowick, M. J.; Cacciuto, A.; Dinsmore, A. D.; Hsu, M. F.; Nelson, D. R.; Nikolaides, M. G.; Travesset, A.; Weitz, D. A. *Science* **2003**, *299*, 1716−1718.
(3) Binks, B. P.; Murakmi, R. *Nat. Mater.* **2006**, *5*, 865−869.
(4) Euler, L. *Opera Omnia*, series i, Vol. 26; Orell Füssli Verlag: Zurich, Switzerland, 1953.
(5) Hilton, P.; Pedersen, J. *Am. Math. Month.* **1996**, *103*, 121−131.
(6) Thomson, J. J. *Philos. Mag.* **1904**, *7*, 237−265.
(7) Einert, T.; Lipowsky, P.; Schilling, J.; Bowick, M. J.; Bausch, A. R. *Langmuir* **2005**, *21*, 12076−12079.
(8) Horozov, T. S.; Binks, B. P. *Angew. Chem., Int. Ed.* **2006**, *45*, 773−776.
(9) Binks, B. P.; Murakami, R.; Armes, S. P.; Fujii, S. *Angew. Chem., Int. Ed.* **2005**, *44*, 4795−4798.
(10) Binks, B. P.; Clint, J. H.; Whitby, C. P. *Langmuir* **2005**, *21*, 5307−5316.
(11) Binks, B. P.; Philip, J.; Rodrigues, J. A. *Langmuir* **2005**, *21*, 3296−3302.
(12) Hsu, M. F.; Nikolaides, M. G.; Dinsmore, A. D.; Bausch, A. R.; Gordon, V. D.; Chen, Xi; Hutchinson, J. W.; Weitz, D. A. *Langmuir* **2005**, *21*, 2963−2970.
(13) Cayre, O. J.; Noble, P. F.; Paunov, V. N. *J. Mater. Chem.* **2004**, *14*, 3351−3355.
(14) Noble, P. F.; Cayre, O. J.; Alargova, R. G.; Velev, O. D.; Paunov, V. N. *J. Am. Chem. Soc.* **2004**, *126*, 8092−8093.
(15) (a) Velev, O. D.; Furusawa, K.; Nagayama, K. *Langmuir* **1996**, *12*, 2374−2384. (b) Velev, O. D.; Nagayama, K. *Langmuir* **1997**, *13*, 1856−1859.
(16) Gordon, V. D.; Chen, X.; Hutchinson, J. W.; Bausch, A. R.; Marques, M.; Weitz, D. A. *J. Am. Chem. Soc.* **2004**, *126*, 14117−14122.
(17) Cauvin, S.; Colver, P. J.; Bon, S. A. F. *Macromolecules* **2005**, *38*, 7887−7889.
(18) Bon, S. A. F.; Cauvin, S.; Colver, P. J. *Soft Matter* **2007**, *3*, 194−199.
(19) Fujii, S.; Ryan, A. J.; Armes, S. P. *J. Am. Chem. Soc.* **2006**, *128*, 7882−7886.

10.1021/cm0708362 CCC: $37.00
Published on Web 08/14/2007

Scheme 1. Schematic for Fabricating Polymeric Microparticles of Various Structures.

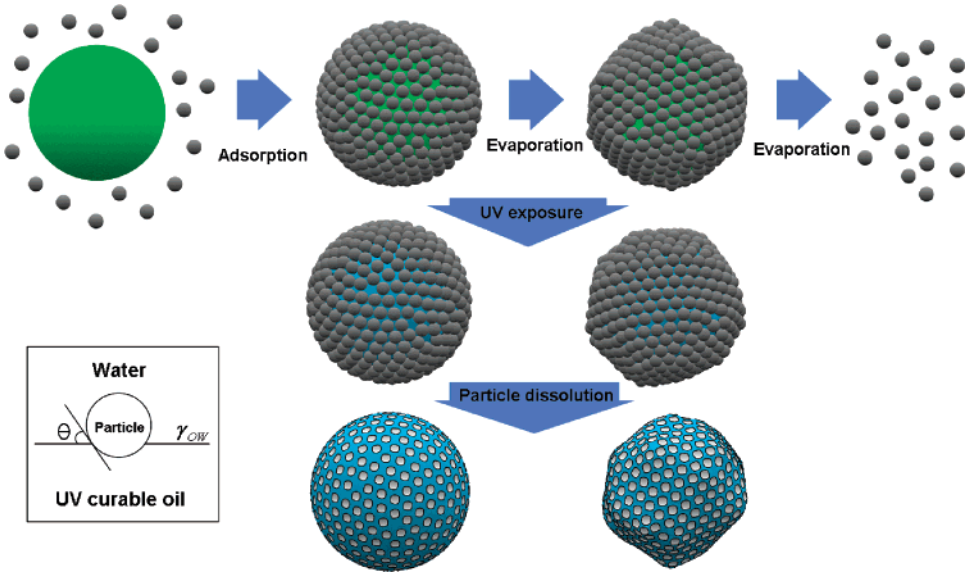

When small stabilizing particles were adsorbed on the surface of a UV-curable oil drop, the particle-covered oil drop was exposed to UV light; subsequently the small particles were removed selectively, leaving behind a dimpled polymeric structure. When a volatile oil was added into the drop phase, buckled structures were produced by evaporation of the volatile oil. The definition of contact angle was schematically shown in the inset.

particle-stabilized emulsions have been developed for superhydrophobic surface with hierarchical topologies.[22] Also, spherical hollow shells of colloidal particles and golf-ball-like structures were prepared by assembling amphiphilic particles of which the surfaces were modified asymmetrically.[23] However, it not yet fully understood how the structural relaxation behavior and mobility of particle-stabilized emulsions are affected by the surface chemistry such as contact angles or binding energies of the colloidal particles bound to the emulsion interface.

In this article, we examined the structural behavior and mobility of Bancroft-type emulsions, which were stabilized by small colloidal particles adsorbed from continuous phase,[24] and developed a simple method for fabricating polymeric particles with complex surface morphologies using a particle-stabilized photocurable emulsion in aqueous medium. Specifically, raspberrylike or golf-ball-like particles were produced with controlled surface morphologies by changing colloidal surface chemistry. To do this, several hydrophobic particles with a contact angle ranging from 30 to 150° were synthesized for the stabilization of the oil-in-water emulsions. The stabilizing particles were much smaller than the emulsion droplets and the size ratio was in the range of 0.001−0.1. Particulate shells were then immobilized by rapid photocuring of the emulsion drop phase to produce polymeric raspberry particles. Subsequently, microparticles with golf ball-like surface morphology were prepared by removing the small particles from the surfaces of the raspberry particles. Recently, Takahara et al. produced similar structures using amphiphilic particles that were prepared by treating the exposed surfaces of the particles at liquid−liquid interface with alkylsilyl groups.[23] However, we used quite different and unique strategy for these structures. In our study, the surfaces of silica particles were modified by adsorbing organosilane, which was added in the dispersion, and the hydrophobic moieties were distributed isotropically. More importantly, we used a UV-curable oil phase with considerably low volatility to immobilize rapidly the particle assembly by UV exposure, which was required for interrogating the fundamental physics of buckling phenomenon and crystallography. The present particle-stabilized emulsions have a few important characteristics; first, the small particles bound to the interfaces not only made the emulsion droplets stable but tended to keep the emulsion droplets from deforming. Therefore, the emulsion droplets elongated under the action of viscous shearing force would not relax back to spherical shape but sustain the elongated shape after the shearing force was released. Although Stone et al. and Binks et al. investigated particle-stabilized nonspherical bubbles and emulsion drops, they did not characterize the interface shapes and properties.[3,25] Second, the degree of the interface immobilization could be controlled by modifying the surface properties of the stabilizing particles such as contact angle or interfacial binding energy. Third, by using a mixture of volatile hydrocarbon oil and UV-curable resin as the oily droplet phase, we could capture a certain state of buckled particle-stabilized emulsion, which was formed after the prescribed volatile oil was completely evaporated (see Scheme 1). According to our observation, separated 5-fold defects become vertices of polyhedron structure, whereas 6-fold particles form faces. The present method for capturing

(20) Binks, B. P.; Horozov, T. S. *Angew. Chem., Int. Ed.* **2005**, *44*, 3722−3725.
(21) Evans, C. C.; Zasadzinski, J. *Langmuir* **2003**, *19*, 3109−3113.
(22) Benkoski, J.; Hu, H.; Karim, A. *Macromol. Rapid Commun.* **2006**, *27*, 1212−1216.
(23) (a) Takahara, Y. K.; Ikeda, S.; Isohino, S.; Tachi, K.; Ikeue, K.; Sakata, T.; Hasegawa, T.; Mori, H.; Matsumura, M.; Ohtani, B. *J. Am. Chem. Soc.* **2005**, *127*, 6271−6275. (b) Takahara, Y. K.; Ikeda, S.; Tachi, K.; Sakata, T.; Hasegawa, T.; Mori, H.; Matsumura, M.; Ohtani, B. *Chem. Commun.* **2005**, 4205−4207.
(24) Golemanov, K.; Tcholakova, S.; Kralchevsky, P. A.; Ananthapadmanabhan, K. P.; Lips, A. *Langmuir* **2006**, *22*, 4968−4977.
(25) Subramaniam, A. B.; Abkarian, M.; Mahadevan, L.; Stone. H. A. *Nature* **2005**, *438*, 930.

the structures of buckled emulsions at a certain state by using mixture of a volatile oil and a nonvolatile photocurable resin will provide an important clue for the unsolved problem. Fourth, our solidification process is very simple because we used just UV exposure within 10 s at room temperature for the structural fixation, which is extremely short compared with the times required for the gel trapping of Paunov et al. (about 48 h)[26] and the radical polymerization of Bon et al. (about 20 h).[18]

In the subsequent sections, we described experimental details of the solidified Pickering emulsion and discussed the morphology of the emulsion droplets and resulting photocured microparticles in terms of the types of the small stabilizing particles and the oily emulsion phases. In particular, photocurable oil-in-water emulsions, and their solidifications with spherical or nonspherical shapes were discussed in detail. Finally, the concept for capturing the structures of buckled emulsions at a certain state was outlined.

Experimental Section

Materials. Two kinds of micrometer scale particles were used in this experiment. Bare silica particles of 1.0 and 1.2 μm average diameter, denoted as silica (A) and silica (B), respectively, were synthesized by the seeded growth method. Aqueous suspensions of polystyrene (PS) latex particles 1 μm in diameter were purchased from Interfacial Dynamics. The surfaces of PS particles were functionalized with either sulfate (Interfacial Dynamics, 1−1000) or carboxylate groups (Interfacial Dynamics, 7−1000), which were designated as latex (A) or latex (B), respectively. Ethoxylated trimethylolpropane triacrylate (ETPTA; SR454, Sartomer) and 2-hydroxy-2-methyl-1-phenyl-1-propanone (HMPP; Darocur1173, Ciba Chemical) were used as UV-curable oil and photoinitiator, respectively. Toluene, PS homopolymer ($M_w \approx 32\,660$), and polyvinylpyrrolidone (PVP, $M_w \approx 56\,000$) were purchased from Sigma-Aldrich. Octadecyltrimethoxysilane (OTMOS, Aldrich) was used for the surface modification of the silica particles with chloroform (Aldrich) as a cosolvent and ammonium hydroxide (28%, Junsei) as a catalyst for OTMOS.

Surface Modification of Silica Particles. To control the hydrophobicity of the silica particles, we anchored organosilane to their surface following the procedures described in a previous report.[27] Specifically, 46.5 mL of ethanolic suspension of silica (A) and 1.75 mL of ammonia (28%) were mixed thoroughly by gentle stirring. Then, 2.5 mL of 10 wt % OTMOS in chloroform was prepared and added dropwise into the mixture of silica suspension and ammonia. The silica suspension was then stirred for 2 h and the silica particles were redispersed in water. The resulting surface-modified silica particles were denoted as silica (E). To differentiate the hydrophobicity of the silica particles, the concentration of the silica suspension and the amounts of organosilane and other chemicals were varied. For example, silica (D) that was 1 μm in diameter was slightly less hydrophobic than silica (E) of the same size, because the concentrations of organosilane and other chemicals were one tenth of those for silica (E). Similarly, we prepared various silica particles, silica (C−G), with different surface properties, and the physical properties of the prepared silica particles and PS latex particles (latex (A) and (B)) are shown in Table 1. In the present case, the zeta potentials of silica particles ranged from −51.2 to −64.0 mV and −57.2 and −77.5 mV for polystyrene latex particles with sulfate and carboxylate groups, respectively. These zeta potentials were higher than the rough guideline for stability, −30 mV. Indeed, most silica and polystyrene particles used in this paper were stable in the aqueous phase and strong enough for the well-ordered arrangement of particles on emulsion interface.

Table 1. Contact Angles, Binding Energies, and Diameters of the Stabilizing Silica and PS Particles

samples of particles	diameter (μm)	contact angle ($^\circ$ θ)	surface group	binding energy (E_b/kT)
silica (A)	1.00	0	hydroxyl	less than O(10)
silica (B)	1.20	0	hydroxyl	less than O(10)
silica (C)	1.20	33	octadecyl	6.1×10^4
silica (D)	1.00	60	octadecyl	4.1×10^5
silica (E)	1.00	90	octadecyl	1.6×10^6
silica (F)	0.25	120	octadecyl	2.5×10^5
silica (G)	0.20	36	octadecyl	2.4×10^3
latex (A)	1.00	110	sulfate	7.0×10^5
latex (B)	1.00	150	carboxyl	2.9×10^4

Preparation of Emulsion Droplets and Solidification by UV Exposure. We used three different oil phases to prepare oil-in-water emulsions; namely, toluene, ETPTA, and a mixture of toluene and ETPTA with a fraction of toluene at 20 wt %. For toluene-in-water emulsion, 0.08 wt % PVP was used as an additional stabilizer. When UV-curable ETPTA was used for the oil phase, no additive was used except HMPP as a photoinitiator. Oil-in-water emulsion droplets were formed by shearing a mixture of the oil phase (500 μL) and aqueous suspension (6 mL) of silica or PS particles at 16 000 rpm for 1 min. The oil droplets were in the range of 10−100 μm in diameter and much larger than the stabilizing particles. The mixture of emulsion droplets and stabilizing particle suspension was then kept in a closed vial for 24 h, which was sufficiently long for the particles to be adsorbed over the entire emulsion interface. In doing this, Pickering emulsions were spontaneously formed, as the emulsion droplets were decorated with hydrophobic silica, sulfate-terminated PS, or carboxyl PS. To instantly capture the morphology of the particle-stabilized emulsion droplets, we exposed the emulsion directly to a broad UV light (mercury arc lamp) for 10 s. The UV-cured ETPTA droplets held the particles at their surfaces.

Characterization. Images of the particle-stabilized emulsions were taken with an optical microscope (Nikon, TE2000-U and L150). The UV-cured microparticles with 2D surface-packed small particles were observed via scanning electron microscopy (SEM) (Philips XL30). To do this, the samples were coated with Au to render them conductive. Typically, the acceleration voltage for SEM was 3−10 kV.

Results and Discussion

It is well-known that emulsions can be stabilized with small amphiphilic particles that are bound to the interface.[28] The mechanism by which particles stabilize the so-called Pickering emulsion involves a reduction of the total surface energy by decreasing the area of the free interface when particles are adsorbed at oil−water interface.[29] The interfacial energy reduction by particle anchoring is expressed as

$$E_b = \pi R^2 \gamma_{ow}(1 - |\cos\theta|)^2 \quad (1)$$

where R is the particle radius, γ_{ow} the interfacial tension, and θ the contact angle measured from the water phase.

(26) (a) Cayre, O. J.; Paunov, V. N. *Langmuir* **2004**, *20*, 9594−9599. (b) Paunov, V. N. *Langmuir* **2003**, *19*, 7970−7976.
(27) Wang, W.; Gu, B.; Liang, L.; Hamilton, W. *J. Phys. Chem. B* **2003**, *107*, 3400−3404.
(28) Pickering, S. U. *J. Chem. Soc.* **1907**, *91*, 2001.
(29) Binks, B. P.; Lumsdon, S. O. *Langmuir* **2000**, *16*, 8622−8631.

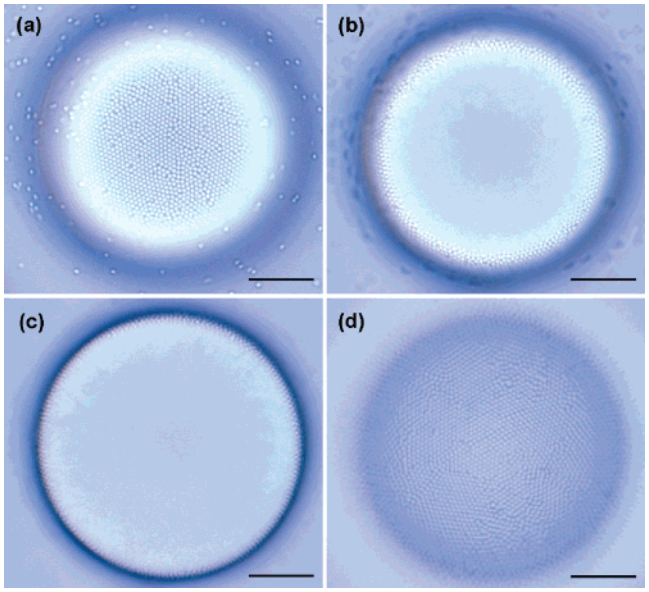

Figure 1. Optical microscope images of a toluene drop covered with slightly hydrophobic Silica (C) particles 1.2 μm in size. The images were taken in the focal plane of (a) near the bottom, (b) slightly above the bottom, (c) in the middle, and (d) on top of the drop. The particles were well-packed and formed a spherical shell. The scale bar is 20 μm.

Because this expression is obtained by considering the energy difference between the nonadsorbed state and adsorbed state, E_b in eq 1 can be considered as being the "binding energy", i.e., the energy that must be overcome to remove one particle from the interface into either the water phase when $\theta < 90°$ or the oil phase when $\theta > 90°$. Notably, we neglected the contribution from the curvature effect of the emulsion interface in eq 1, because the emulsion droplet was so large that the ratio of particle to emulsion drop size was kept in the range of 0.001−0.1. The contact angles θ on various silica and PS particles were measured from the particle-straddled interface shapes, and the results are shown in Table 1. Also included in Table 1 are the binding energies per particle, which were estimated using eq 1 with the interfacial tension $\gamma_{ow} = 8.5$ mN/m between ETPTA and water as provided from Sartomer. For $\theta < 10°$ or $\theta > 170°$, the magnitude of the binding energy (E_b) is the order of thermal energy for submicrometer particles, and these particles cannot be bound firmly to the interface because of thermal Brownian motion. Therefore, bare silica particles with $\theta < 10°$ were not likely to adsorb on the interface unless their surfaces were properly modified to induce a certain level of hydrophobicity. In the following sections, we described the fabrication of self-organized structures using surface-modified silica particles and PS latex particles, as illustrated in Scheme 1.

Toluene Droplets Covered with Silica Particles in Water. Hydrophobic silica (C) particles were adsorbed at the interface of toluene droplets in water. The particles were well-packed and formed a spherical shell. As shown in different focal planes of Figure 1, the silica particles were not present inside the droplets but arranged hexagonally on the oil−water interface with inevitable defects on spherical surface packing. In this case, the optical micrographs can be used as an ideal model for spherical crystallography for analyzing the surface arrangement of particles or Delaunay triangulation.[30] However, the particle-covered toluene emulsion droplet could not keep its structure, as toluene evaporated and diffused slowly into ambient air through the aqueous medium. The structural evolution can be seen clearly from Figure 2, in which optical microscope still-shot images of a particle-stabilized toluene drop were reproduced at different evaporation times. As the toluene droplet became smaller, the particle shell on the interface began to crumple and lose the spherical shape. The interface distortion was due to the fact that the anchored particles were likely to be bound to the interface and needed the same interfacial area even though the volume of emulsion drop decreased by evaporation. Consequently, the interface was highly distorted by the attached particles, thereby inducing higher surface energy (or larger interfacial area) per unit volume of the emulsion droplet. In the final stage of evaporation, some of the particles were forced out of the interface because van der Waals attraction could not overcome repulsive excluded volume and electrostatic interactions. Overall, spherical emulsion droplets at the initial state were abruptly transformed into irregularly folded shapes via faceted structures within 1 min. Finally, the folded structures fell apart and the particles were released to the continuous phase without any trace of the particle structures.

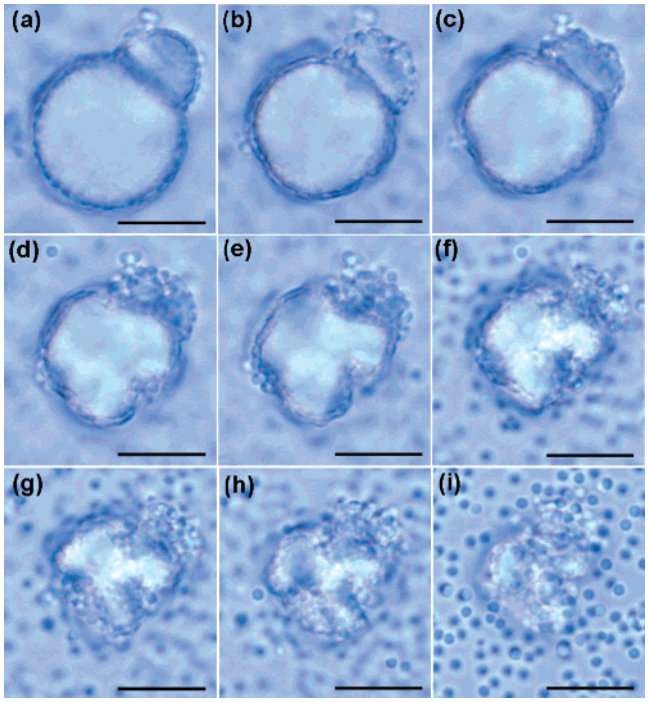

Figure 2. Optical microscope images of a toluene covered with silica (C) particles taken in an open bath with a time interval of about 10 s. The structural evolution started from (a) spherical shape to (f) crumpled shape. Eventually, the particle structure disappeared (g−i) as toluene evaporated completely. The scale bar is 10 μm.

To maintain a crystalline monolayer of small particles anchored on the emulsion drops, several groups have attempted to make a rigid shell, in which latex particles were bonded by annealing or chemical reactions.[1,12−18] Resulting hollow structures after removal of the emulsion phase are potentially useful for encapsulating target materials. Here,

(30) Delaunay, B. Bull. Acad. Sci. USSR Class. *Sci. Math. Nat.* **1934**, *7*, 793−800.

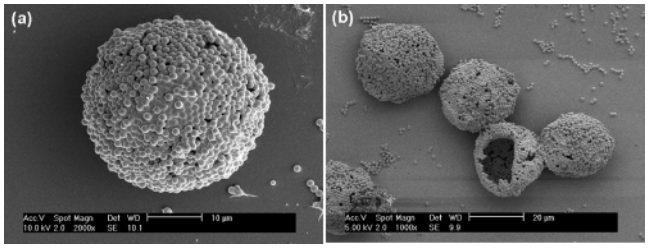

Figure 3. (a) SEM image of PS microparticle covered with silica (C) particles formed by evaporating toluene containing 15 wt/wt % PS homopolymer (M_w = 32 660). (b) SEM image of hollow colloidal shells produced by thermal decomposition of PS from the composite structures of (a). The scale bars in (a) and (b) are 10 and 20 μm, respectively.

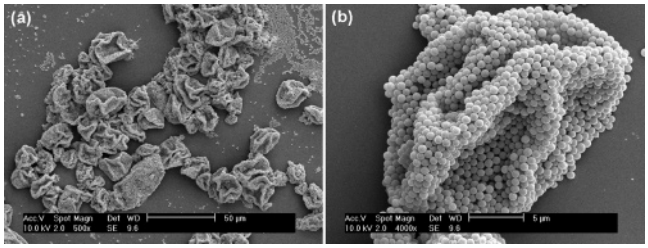

Figure 4. (a) SEM image of folded PS structures covered with silica (C) particles produced by evaporating toluene containing 3 wt/wt % PS homopolymer (M_w = 32 660). (b) Magnified SEM image of (a). The scale bars in (a) and (b) are 50 and 5 μm, respectively.

unlike the previous method reported by Velev et al. in which macromolecules were introduced from a continuous phase to induce additional reaction for fixing the structure,[15] we dissolved PS homopolymers (M_w = 32 660) in the drop phase of toluene in order to keep the colloidal structure at the emulsion interface. The emulsion drop became viscous and finally solidified as the toluene evaporated. Similarly, Weitz et al. produced composite capsules from PS particle-stabilized emulsion drops networked by polymer chains in the aqueous emulsion phase.[16] However, they used phase inverted water-in-oil emulsion and did not make dried capsules because the method was not based on the evaporation of emulsion phase. Using 15 wt % PS homopolymers in toluene as a droplet phase, particle-stabilized emulsions were successfully produced and particle-decorated "raspberry" microparticles were produced after complete evaporation of toluene, as shown in Figure 3a. Subsequently, by burning out PS homopolymers at 500 °C, hollow colloidal shells were obtained, as shown in Figure 3b. When the content of PS homopolymers was as low as 3 wt % in toluene phase, crumpled structures were formed instead of spherical shells, as shown in Figure 4. This is because the adsorbed polymer layer formed at this low concentration could keep the particles from being disassembled but the particle structures were not strong enough and buckled during the evaporation of toluene.

UV-Curable Emulsions Stabilized with Monodisperse Particles. Because toluene droplets rose to the free surface because of low specific gravity, the stabilizing particles did not have enough time for complete coverage by adsorption on the emulsion interfaces before they reached the free surface. Under this condition, the emulsion drops were covered partially and colliding among others near the free surface, which induced coalescence. This was especially true of larger emulsion drops stabilized by particles with lower contact angles. To avoid this problem as well as fast shrinkage of the emulsion droplets caused by evaporation of toluene, we used UV-curable prepolymers (ETPTA) as a droplet phase instead of toluene. Because of its relatively high specific gravity (1.11 at 25 °C) and low volatility, ETPTA drops were highly stable when fully covered with hydrophobic silica particles. Subsequently, UV-induced polymerization transformed the emulsion droplets into solid microparticles that tethered the small particles on their surfaces. It is noteworthy that the volume of ETPTA monomer decreased slightly by 4% during polymerization[31] and the degree of deformation was trivial. If an ETPTA droplet was spherical initially and covered with non-close-packed colloidal silica spheres, its shape remained spherical with the diameter reduced only by 1.35%. For an ETPTA drop that was initially spherical and covered with close-packed silica spheres, the drop should be deformed slightly to keep the surface area unchanged during the volume shrinkage. Also, we calculated the asphericity of particle-stabilized emulsion droplet using Surface Evolver, which has been used for predicting the shape of interface by minimizing the total free energy.[32] The asphericity is zero when the structures are perfectly spherical. In the present case, the asphericity was increased slightly from 2.33×10^{-5} to 9.28×10^{-5} for 4% volume shrinkage during UV-induced consolidation of ETPTA. Therefore, no appreciable deformation of the emulsion droplets occurred during UV curing.

To examine the effect of the surface modification of small stabilizing particles on the structure of emulsion droplets, we used various silica particles with different contact angles or hydrophobicities as stabilizing particles. The hydrophobicity became larger in the order of silica (A) $\approx$ silica (B) $<$ silica (C) $<$ silica (D) $<$ silica (E) for micrometer-scale particles. Consequently, the binding energy was increased in the same order. For sub-micrometer-scale particles, the binding energy of silica (F) was much larger than that of silica (G). If the silica particles did not possess hydrophobic moiety on the surface like silica (A), they could not be adsorbed on the emulsion droplets. In this case, as shown in images a and b of Figure 5, smooth spherical polymeric particles with no dimples were produced upon UV irradiation over the ETPTA drops, which were emulsified in aqueous suspension of the bare silica particles. In contrast to the bare silica (A), however, slightly hydrophobic silica (C) particles covered fully the ETPTA droplets and stabilized the ETPTA-in-water emulsion even though they possessed only weak hydrophobicity. The particle-stabilized emulsion droplets were solidified via UV exposure, as shown in images c and d in Figure 5. It should be noted that when silica (C) particles formed a compactly packed monolayer on the interface, stabilizing the emulsion droplets, the particle-anchored interface would not be deformed during UV exposure or under the external disturbances. Because the particle-covered emulsions do not change their configuration under external disturbances, they would be an ideal model to study spherical crystallography. When microparticles are dried out on a

(31) Jiang, P.; McFarland, M. J. *J. Am. Chem. Soc.* **2004**, *126*, 13778−13786.
(32) (a) Brakke, K. A.; *Exp. Math.* **1992**, *1*, 141. (b) Lauga, E.; Brenner, M. P. *Phys. Rev. Lett.* **2004**, *93*, 238301.

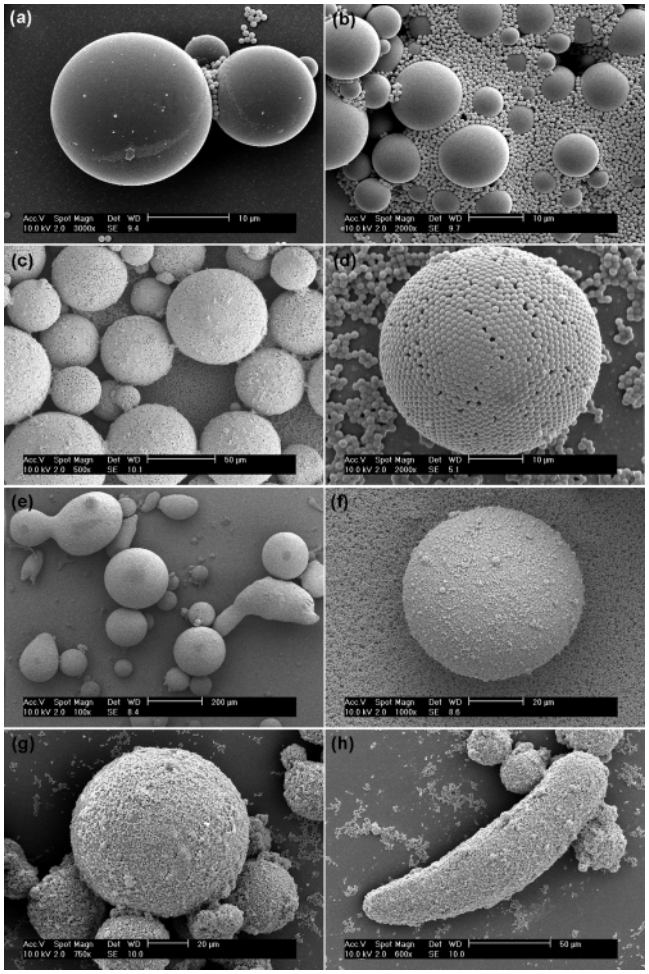

Figure 5. (a,b) SEM images at different magnifications of UV-cured polymeric microparticles, which were produced from ETPTA drops dispersed in an aqueous suspension of the bare silica (A) particles. The silica (A) particles were detached from the polymeric microparticles after UV curing, leaving behind no dimples. (c, d) SEM images at different magnifications of UV-cured polymeric microparticles covered with slightly hydrophobic silica (C) particles. (e, f) and (g, h) SEM images at different magnifications of UV-cured polymeric microparticles covered with hydrophobic silica (D) and silica (E) particles, respectively.

substrate, the configuration of small particles on the surface of a microparticle can be observed via electron or optical microscopy from various viewing angles, which is particularly useful for defect analysis with colloids in spherical crystallography. According to Bausch et al., the imaged surface area is between 5 and 20% of the full surface area of the emulsion, depending on the size of the droplet.[2] However, the imaged surface area would be 100% by rolling the sphere or at least 80% by tilting the angle of observation.

Also, we attempted to stabilize the ETPTA-in-water emulsions using hydrophobic silica (D) particles. In this case, a variety of spherical and nonspherical elongated or wormlike microparticles were produced as shown in Figure 5e, which was distinctively different from images c and d in Figure 5 for less hydrophobic silica (C) particles. The SEM image in Figure 5f of the photocured microparticles showed that the microparticles were covered mainly with monolayer of silica (D) particles, and locally double layers were formed. For silica (E) particles, which were slightly more hydrophobic than silica (D), spherical and nonspherical microparticles with multilayered stabilizing particles were generated, as shown in images g and h in Figure 5. These multilayers are caused by preaggregation due to the instability in the aqueous phase, which is caused by the high density of the hydrophobic moiety. Nonspherical bubbles and emulsion drops have been reported in a recent study by Stone et al., in which they speculated that such nonspherical bubbles and emulsions were formed because of the particles jamming on the interface.[25] However, according to our experimental results, a jammed shell did not always produce nonspherical emulsions; only 1 μm particles of silica (D) and silica (E) consistently produced nonspherical emulsions. Notably, the main characteristic difference of the particles was the contact angle or binding energy at ETPTA−water interface, i.e., the contact angles were 33, 60, and 90° for silica (C), silica (D), and silica (E), respectively. Therefore, the particle's capacity to support unequal stresses was related to the contact angle. In particular, the emulsion droplets stabilized with silica (E) particles would not be relaxed to a spherical shape from a nonspherical deformed shape under the action of external flow or electric field for a few days after the external field was removed. Otherwise, the same emulsion droplets without stabilizing particles would regain the spherical shape instantly. The estimated relaxation time scale ($\eta R_d/\gamma_{ow}$) for an emulsion droplet of diameter R_d and viscosity η was in the order of 1×10^{-3} s for a clean and mobile emulsion interface with $R_d = 100$ μm. The same mechanism could be applied to nonspherical bubbles.

The mobility of the particle-straddling interface can be explained by considering the capillary forces as the binding force for keeping the particles at the interface after adsorption. As obvious from eq 1, low-contact-angle particles such as silica (C) had relatively weak binding energy and could not cover the interface compactly at the initial stage. Moreover, thermal fluctuations released some adsorbed particles from the interface to the continuous phase and the particle adsorption at the interface was reversible because of their low binding energy compared to the particles at the free surface of air bubble. Therefore, although nonspherical emulsion drops were formed during the shearing process of emulsification, noneven stress was not sustained because the interfacial jamming of particles was insufficient with small contact angles. Even after the spherical shape of the emulsions was restored, the emulsion interface was not saturated and more particles were able to adsorb on the drops. In contrast, strongly adsorbed particles such as silica (E) with high binding energy with contact angle $\theta \approx 90°$ kept the nonspherical emulsion drops, which were formed at the initial emulsification stage, from being relaxed to spherical shape because two-dimensional jamming of the particles with strong binding energy made the interface immobile, supporting unequal nonisotropic stresses.

After the emulsion drops were solidified by UV exposure, the particulate silica shells of the photocured polymeric particles were removed easily by chemical etching, which left behind golf-ball-like dimpled particles. Here, we dissolved the silica particles using 0.6 wt % NaOH solution without deforming the polymeric particles. Arrays of hemispherical dimples were templated on the surface of the polymeric microparticle as shown in the SEM images of

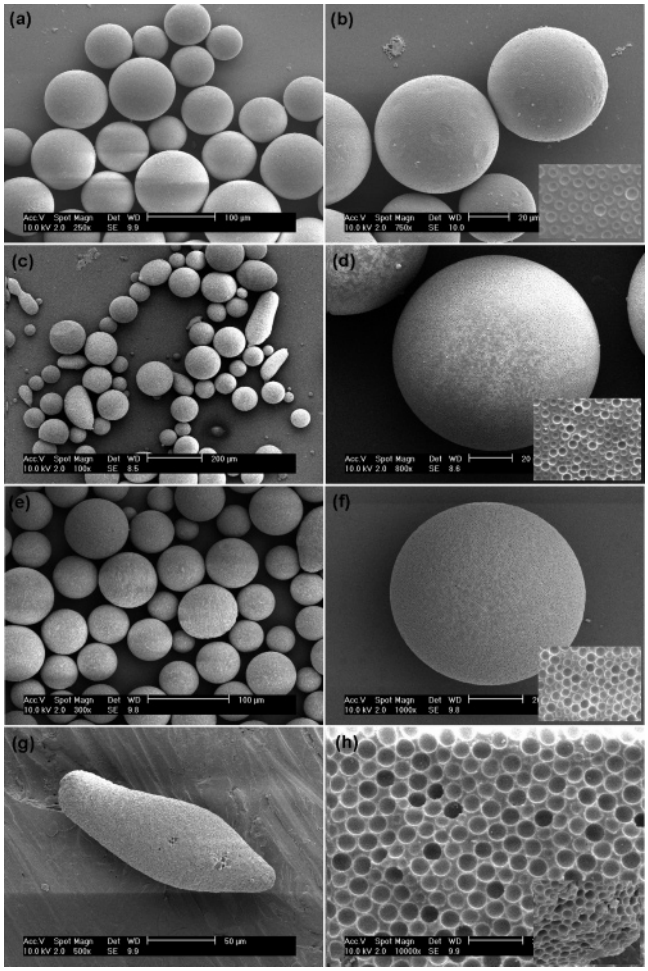

Figure 6. SEM images at different magnifications of golf-ball-like structures; (a, b) with shallow and small dimples left behind by slightly hydrophobic silica (C); (c, d) with deeper and larger dimples by hydrophobic Silica (D); (e, f) with deepest and largest dimples by more hydrophobic Silica (E). (g, h) SEM images at different magnifications of nonspherical microparticles produced with Silica (E); (h) was taken from a small curvature region with the inset from an edge region.

Figure 6. The morphology of these dimples provides important information on the trace of particle adsorption. When the adsorbed particles do not disturb the interface, the open circle diameter (D) of the dimples templated from the particles can be related to the contact angle of the particles as follows

$$\sin\theta = \frac{D}{2R} \tag{2}$$

in which R and θ are the radius of the particle and the contact angle, respectively. Therefore, given the particle size, we can indirectly calculate the contact angle θ from the open circle diameter (D) of the dimples. The present method for measuring the contact angle is conceptually similar to the method developed by Paunov et al. using gel trapping, but much clearer because removal of the particles provides completely the traces of the particles.[26] In the present study, the estimated contact angle of silica (C) particle was 33° on the basis of the averaged dimple size (standard deviation 6°) from the SEM images of the dimpled polymer particles in Figure 6b. Similarly, the contact angles θ of silica (D) and silica (E) particles were estimated from the corresponding

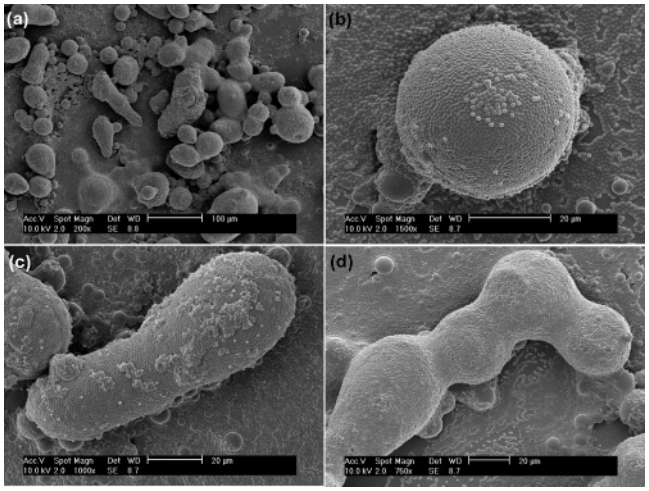

Figure 7. (a−d) SEM images at different magnifications of UV-cured ETPTA microparticles covered with latex (A) particles. Various spherical and nonspherical particles were produced from the ETPTA emulsion drops immobilized by latex (A) particles with strong binding energy.

SEM images of the dimpled surfaces in the insets of images d and f in Figure 6, and the results are $\theta = 60°$ (standard deviation 12°) and 90° (standard deviation 15°), respectively. In particular, the magnified SEM image for which $\theta = 90°$ showed that a silica (E) particle was straddling on the interface with one-half in the oil phase and the other in aqueous continuous phase. Comparison of the SEM images in the insets of images b, d, and f in Figure 6 showed that the size or depth of the dimples was increased with the contact angle ranging from 33 to 90°. As noted from the insets of images b, d, and f in Figure 6, the size of the dimple was nonuniform, which was due to the uneven hydrophobic surface. SEM images g and h in Figure 6 show nonspherical particles of which the surfaces were covered with hemispherical dimples. Unlike the image in Figure 6h taken from a small curvature region of nonspherical surface, the inset of Figure 6h shows a nonhexagonal and highly distorted interface near the sharp edge of the nonspherical surface. Inevitably, a distorted small-curvature interface produced highly nonuniform stresses, which would have been relaxed by restoring spherical shape without the stabilizing particles. However, when the stabilizing particles were present with $\theta \approx 90°$, the compactly packed emulsion interface became almost immobile and could sustain a highly distorted shape.

Although more hydrophobic silica particles could be produced by additional reaction of OTMOS, the dispersion stability in aqueous medium was poor and stable emulsions could not be obtained. Therefore, instead of silica particles, more hydrophobic PS particles were used for stabilizing oil-in-water emulsions. Usually, PS particles are highly stable in the aqueous phase because of the presence of tethered functional groups. However, a large portion of the surface still contains a hydrophobic moiety because of the intrinsic characteristics of PS.[15] Using sulfate-terminated PS particles (henceforth, latex (A)), we successfully prepared particle-stabilized ETPTA-in-water emulsions. Subsequently, UV exposure produced polymeric microparticles of which the small PS particles were partially immersed over the surfaces as shown in Figure 7a−d. In this case, the contact angle of latex (A) particles was approximately 110° and the binding

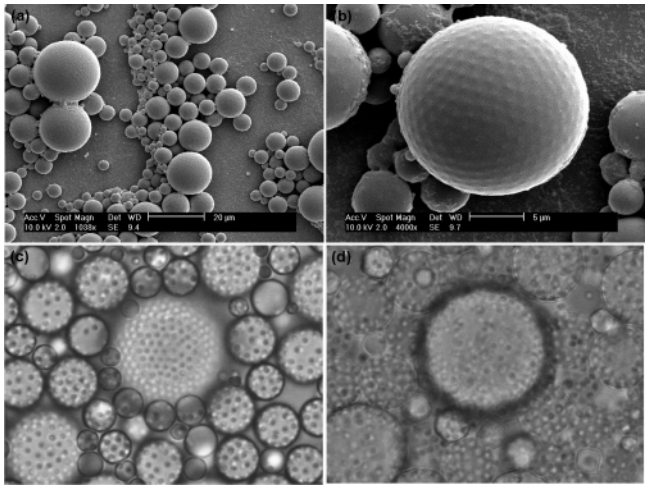

Figure 8. (a, b) SEM images at different magnifications of UV-cured ETPTA microparticles with embossed surface morphology produced from latex (B) particles. (c, d) Optical microscope images taken in different focal planes.

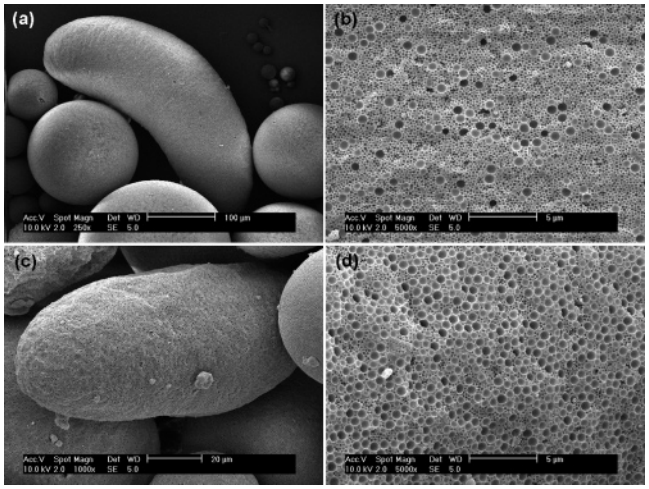

Figure 9. SEM images of UV-cured ETPTA microparticles with bidisperse dimples: (a, b) produced from 250 nm silica (F) and 1 μm silica (D) particles; (c, d) produced from 250 nm silica (F) and 1 μm silica (E) particles. The magnified images in (b) and (d) clearly showed the difference in the surface arrangements of small and large dimples.

energy was slightly lower than the uppermost of silica (E) particles. In Figure 7a, particle-covered polymeric microparticles showed nonspherical or fused shapes, which was similar to the case of silica (D) particles. Higher-magnification images of the spherical and nonspherical microparticles were shown in Figure 7b−7d, respectively. As in the case of hydrophobic silica (D) particles, the sulfate-terminated PS particles were covered with monolayers and double layers of the small PS particles. On the other hand, for PS particles with carboxyl groups (latex (B)), all microparticles were almost spherical in shape and the majority of PS particles were fully immersed in the emulsion drop phase, as shown in Figure 8a and 8b. To investigate whether the embossed structure was caused by the immersed particles or interfacial instability such as Rayleigh−Taylor or Plateau−Rayleigh instability, we examined the optical microscope images, shown in images c and d in Figure 8. Two optical micrographs were taken in different focal planes, revealing that the embossed structure was caused by the fully immersed PS particles rather than by the interfacial instability. The microscope image showed that PS particles are not only on the interface but also inside the emulsion phase. It can be noted from Table 1 that the binding energy of latex (B) was much smaller than that of silica (E), although the contact angle was much larger. Because of the weak binding energy with a large contact angle, latex (B) particles were much more likely to escape from the interface and reside in the oil phase, eventually producing the spherical microparticles with embossed surface morphology.

Now, the effect of the binding energy or contact angle on the emulsion structures and the resulting shape of microparticles can be summarized as follows. When the binding energy was low (i.e., $\theta < 50°$ or $\theta > 130°$), only spherical-shaped microparticles are produced. For $50° < \theta < 130°$, however, nonspherical as well as spherical microparticles are produced. Particles with large binding energy tend to strongly resist rearranging their packing structures on the interface, and the emulsion interface becomes highly immobile. Therefore, the emulsion droplets stabilized by the particles with large binding energy will not be restored to a spherical shape from a nonspherical deformed shape after the removal of shearing force that was applied for emulsification. In particular, particles with the contact angle around $\theta \approx 90°$ have the largest binding energy and can withstand highly nonuniform stresses exerted on nonspherical emulsion interface. The mobility of the emulsion interface is also affected by the reduction of the interfacial area because of the particle adsorption. The ratio (A) of the interfacial area of the particle-decorated emulsions relative to the particle-free emulsions is expressed as

$$A = 1 - \frac{2\pi(R \sin\theta)^2}{6\sqrt{3}R^2} = 1 - 0.6046 \sin^2\theta \qquad (3)$$

in which it is assumed that the particles are arranged hexagonally and the curvature effect of the emulsion interface is ignored. Obviously, as the interfacial area reduction becomes large, the energy gain for the transition from nonspherical to spherical shape decreases. Notably, the interfacial area reduction as a function of the contact angle has the same trend as the binding energy. When the equators of the particles are straddled on the interface (i.e., for $\theta \approx 90°$), the oil−water interfacial area is minimized and about 60% of the interface is occupied by the particles. Indeed, this is consistent with the fact that nonspherical shape was dominant in emulsions for particles with $\theta \approx 90°$.

UV-Curable Emulsions Stabilized with Bidisperse Particles. For a shell of colloidal particles with bimodal size distribution, a 0.6 mL suspension of hydrophobic 250 nm silica (F) particles with 2 wt % and a 6 mL suspension of 1 μm silica (D) particles were mixed and added into an oil−water mixture. In the binary silica suspension, the number of small particles is approximately 6.4 times larger than the number of large particles. The contact angle of 250 nm silica (F) was approximately 120° at the water−oil interface. Bidisperse hydrophobic silica particles were adsorbed competitively at the interface and then etched out to produce complex dimple array on the surface of the photocured polymer particle. As shown in images a and b in Figure 9,

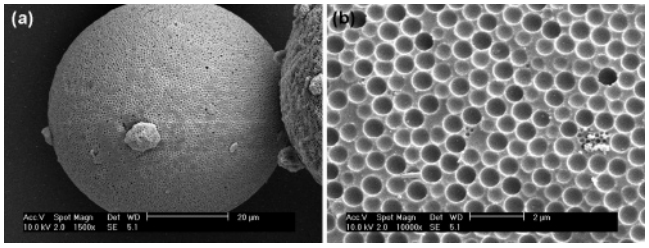

Figure 10. SEM images of UV-cured ETPTA microparticles with bidisperse dimples produced from 200 nm silica (G) and 1 μm silica (E) particles. The magnified images in (b) clearly showed that mainly monodisperse large dimples were formed.

small and large dimples ranging from 250 nm to 1 μm in size were distributed randomly. However, for 250 nm silica (F) particles and 1 μm silica (E) particles, nearly closely packed large dimple arrays were produced with small dimples at their interstices, as shown in images c and d in Figure 9. From the image analysis of Figure 9b, we found that the number of small dimples is 23.7 times larger than the number of large ones. As noted from Table 1, the binding energy of 1 μm silica (D) particles was comparable to that of 250 nm silica (F) particles. Therefore, these binary particles had approximately equal capabilities to retain their occupancies on the interface. However, because of higher mobility of the small particles, silica (F) particles were dominantly adsorbed on the interface, which was responsible for the coarse and random distribution of large dimples in images a and b in Figure 9. Meanwhile, 1 μm silica (E) particles had about 7 times larger binding energy than silica (F) and hence they were more likely to reside on the interface, which produced close packing of large dimples on the interface as shown in images c and d in Figure 9. Here, the number of small dimples was just 3.2 times larger than the number of large ones. As expected, when small particles had considerably small binding energy, such as silica (G) compared to large particles like silica (E), the binary colloids produced polymeric particles on which mainly large dimples were closely packed with a few small scattered dimples, as shown in images a and b in Figure 10.

Our method for synthesizing particles with complex surface morphology is very useful in that the length scales for resulting polymeric particles, and dimples can be controlled readily and independently by changing the contact angles and the sizes of emulsion drops and stabilizing particles. Moreover, the geometry of nonspherical emulsion drops can be controlled using elaborating devices such as four-roll flow devices[33] or electrohydrodynamic flow devices.[34] These flow devices enable precise control of the size and aspect ratio of nonspherical emulsion drops and the resulting polymeric particles with multiple-scale surface patterns.

Particle-Stabilized Emulsion of a Mixture of Toluene and ETPTA. As illustrated in Scheme 1, the interface buckling occurs when the emulsion droplets shrink sufficiently so that the surface density of the particles would be supersaturated if the emulsion drops remained spherical. To examine the buckling phenomena, we added toluene into the oil (ETPTA) phase for the evaporation-induced shrinkage, and the buckled interface was captured by the UV-cured polymerization of ETPTA. By doing this, we could observe the shape of the interface directly after dissolving the stabilizing silica particles. The result showed that the volumetric ratio of volatile toluene to ETPTA determined the buckling state. Here, we used a mixture of 80 wt % ETPTA and 20 wt % toluene with a 1.2 μm silica (C) suspension. Microparticles in Figures 11a showed the particle-decorated polymeric structures, which were produced by UV exposure of the emulsion after toluene was evaporated completely for 8 h at room temperature. The surface morphology of the emulsion interface can be seen from the SEM images of Figure 11b for the polymeric structures obtained after the silica particles were etched out. Interestingly, when toluene was completely removed from the oil-drop phase, faceted polyhedral microparticles were produced. The faceted polyhedral structures can be confirmed from the optical microscope images of Figure 12 in different focal planes, which were taken before UV exposure. Although Fuller et al. reported buckling of solid-stabilized air drops, the relationship between buckling and defect structure is still an unsolved problem.[35] Therefore, the dimpled surface as a replica of the particle-straddled interface shown in Figure 11b will provide a key for understanding of buckling phenomena in relation with crystallography.

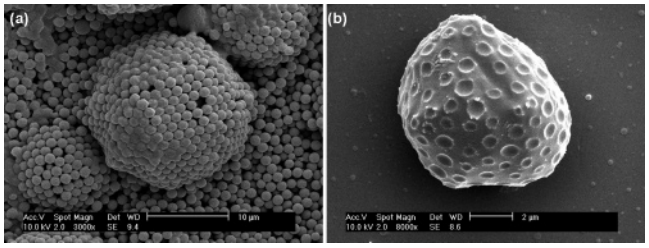

Figure 11. (a) SEM images of faceted polyhedra structures, which were obtained by evaporating toluene completely before UV exposure. (b) SEM images of distorted microparticles with dimples, which were obtained by chemical etching of silica (C) particles from the faceted structure. The dimpled surface is a replica of the particle-straddled interface.

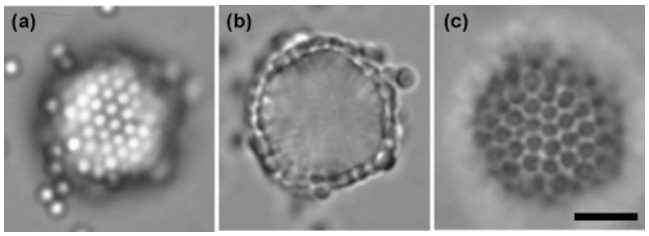

Figure 12. Optical microscope images of ETPTA emulsion drops covered with silica (C) particles. The images were taken after complete evaporation of toluene in different focal planes; (a) near the bottom, (b) in the mid-plane, and (c) on top of the emulsion drop. Faceted edges are clearly seen in (b). The scale bar is 5 μm.

Conclusions

We demonstrated the adsorption and self-assembly of colloidal particles on emulsion interface and in situ capture of emulsion structures by photopolymerization. Using UV-

(33) Bentley, B. J.; Leal, L. G. *J. Fluid Mech.* **1986**, *167*, 219−240.
(34) Ha, J.-W.; Yang, S.-M. *J. Fluid Mech.* **2000**, *405*, 131−156.
(35) Xu, H.; Melle, S.; Golemanov, K.; Fuller, G. *Langmuir* **2005**, 10016−10020.

curable oil, we prepared spherical and nonspherical structures that were composed of a colloidal shell and a polymer core. We also investigated the effect of the contact angle or binding energy of the colloidal particles on the structural relaxation behavior of emulsion drops. Spherical microparticles covered with a shell of close-packed particles are useful for spherical crystallography. In terms of practical applications, these complex structures are also useful for supporting materials of particles with fluorescent dye in a colloidal barcode and for controlling surface roughness of Au-deposited microparticles for surface-enhanced Raman scattering. Using a mixture of volatile toluene and UV-curable oil as an emulsion phase, we could observe the intermediate state of buckling by capturing the structure after complete evaporation of toluene. This could be useful for the study of buckling phenomena by controlling the volume fraction of the volatile oil. Further, golf-ball-like structures were also fabricated by dissolving the particles from the composites of inorganic particle shells and polymeric cores, where the depth and size of the dimples could be controlled by the interfacial characteristics of the particles.

Acknowledgment. This work was supported by a grant from the Creative Research Initiative Program of the Ministry of Science & Technology for "Complementary Hybridization of Optical and Fluidic Devices for Integrated Optofluidic Systems." The authors also appreciate partial support from the Brain Korea 21 Program and thank Prof. Howard A. Stone and his co-worker Anand Bala Subramaniam at Harvard University for helpful discussions on nonspherical Pickering emulsion.

CM0708362